PIOTR BAŃKA [1*], ŁUKASZ SZUŁA [2]

APPLYING SPATIAL STATISTICAL METHODS TO PREDICT GROUND VIBRATION ACCELERATIONS CAUSED BY INDUCED SEISMICITY

This paper presents the results of the research aimed at improving the accuracy of predictions regarding the maximum values of resultant components for horizontal ground vibration accelerations in areas threatened by induced seismicity. The presented solution proposes a spatial model of the ground vibration attenuation relationship based on the assumptions of the Joyner-Boore model. When performing statistical analyses to verify the models, great emphasis was placed on the correctness of applied estimation methods to meet the assumptions. The starting point for introducing spatiality into the models was the occurrence of spatial autocorrelation of the residual component when estimating the structural parameters of a model with the least-squares method. Spatial interactions were presented using weight matrices, the construction of which was based on the inverse of the distance between units. During the study, it was found that the estimated spatial model of the ground vibration attenuation relationship showed a much better match with empirical data compared to the classical Joyner-Boore attenuation model.

Keywords: ground vibration; attenuation relationship; Joyner-Boore attenuation model; spatial statistical methods

1. Introduction

Nowadays, mining operations are more frequently accompanied by rock mass tremors, which, on the one hand, can cause a significant risk to employees and damage to the underground infrastructure of mines and generate noticeable vibrations on the ground surface. Seismicity induced by mining activity is concentrated in Poland around the Legnica-Głogów Copper District and

---

[1]   THE SILESIAN UNIVERSITY OF TECHNOLOGY, FACULTY OF MINING, SAFETY ENGINEERING AND INDUSTRIAL AUTOMATION
[2]   POLSKA GRUPA GÓRNICZA S.A.

*   Corresponding author: piotr.banka@polsl.pl

the Upper Silesian Coal Basin. According to the statistics of the State Mining Authority, 7114 tremors and 11 rock bursts were registered in hard coal mines in the years 2016-2020, as a result of which there were 12 fatal accidents and 2 severe accidents. In the Legnica-Głogów Copper District, 2694 tremors and 12 rock bursts were recorded, which resulted in 10 fatal accidents and 1 serious accident.

While the rock bursts occur relatively rarely in mines, ground vibrations are registered after almost every high-energy tremor. These may cause damage to both public and private buildings as well as technical infrastructure. This is because the tremors cause dynamic loads on buildings designed to withstand solely static loads. For this reason, these dynamic loads can damage buildings, weaken their structure, and reduce their durability and value [1]. The effects of strong vibrations caused by mine tremors on the environment and buildings have been the subject of multiple papers. For example, one can mention the article [2], which analysed the impact of high-energy tremors in two gold mines in South Africa or work [3], in which damage to buildings caused by following high-energy tremors are discussed, highlighting the need for the proper structural design of buildings. However, the most significant consequence of vibrations seems to be the deterioration of living conditions of local communities due to high psychological discomfort [4].

Due to technical and economic reasons, for the most part, it is impossible to register vibration parameters generated by rock mass tremors in all endangered infrastructure facilities. Therefore, industries are required to develop forecasts of surface vibration intensity parameters. However, the estimation of vibration intensity causes many problems. The main reason is that the magnitude of vibrations is determined by several factors, the most important of which are: the seismic energy of a tremor, the hypocentral distance from a tremor source, the source mechanism, and the resulting directionality of vibrations, as well as and the geological structure of the medium affecting the amplification of vibrations [5-7]. In practice, however, predicting the magnitude of vibrations in unobserved objects comes down to determining a relationship between the tremor's seismic energy and the hypocentral distance and the ground vibration parameters [8,9].

This relationship is called the vibration attenuation relationship or ground motion prediction equation (GMPE). Some of the first GMPEs were the models developed by Joyner and Boore [10], Campbell [11] as well as Atkinson and Boore [12]. Local GMPE relations have been developed for practically every seismically active region. A particularly comprehensive review of the above relations is presented in the work [13]. Examples of more complex GMPE relations, taking into account a larger number of parameters, e.g. ground type, sometimes also the mechanism of the shock focus, are the models given in [14-21].

In the literature, the most common proposal for empirical determination of the ground vibration attenuation relationship is the Joyner-Boore model [10].

The estimation of the structural parameters of the GMPE model is the beginning of extensive verification analysis. The accuracy of predictions and the correct construction of confidence intervals for vibration intensity parameters are determined by the statistical verification of estimated parameters, far beyond assessing the significance of the estimates. In fact, the residual component of the model, which affects the form of the variance-covariance matrix, should be extensively analysed [22]. The applied estimation method requires the fulfilment of several assumptions. The estimated model is assumed to be linear regarding the coefficients and error term. The error term is assumed to be independent and identically distributed, i.e. $\varepsilon \sim iid\ (0, \sigma^2 I)$. Moreover, no correlation between explanatory variables is assumed. Furthermore, the exogeneity of explanatory variables requires that variables X are uncorrelated with the error term. Finally, it is assumed that the error term is normally distributed.

When analysing the observational data, there is a recurring phenomenon of spatial autocorrelation of the residual component of the GMPE model estimated by the least squares method is often observed, among other things, such as varied structure and thickness of near-surface layers. This manifests itself in the spatial clustering of residuals of the model estimated by the least squares method. A substantially justified procedure in the face of such a situation is to introduce spatiality into the model, understood as the differentiation of information coming from tremors whose epicentres are at different distances from each other. The application of statistical models of spatial relations of GMPE has been the subject of fewer studies than in the case of the classical approach. As with this approach, the structural parameters are estimated by the method of least squares, and the input data to the model coming from different measuring stations are treated as cross-sectional data. Research into the spatial correlations of recorded ground vibrations has been carried out for two decades. They mainly concern earthquakes [23-25]. The current state of research has been widely discussed in the works [26,27].

This paper presents a method of estimating ground vibration parameters using statistical spatial models applied to data about ground vibrations caused by tremors induced by mining extraction. Such vibrations are characterised by much smaller peak ground acceleration (PGA) and peak ground velocities (PGV) values in comparison to earthquakes.

The analysis of the residual component of the model GPME for the analysed data made it possible to identify spatial autocorrelation of the error term, as well as determine an interaction matrix and estimate the model of vibration attenuation relationship, taking into account the spatial structure of strong rock mass tremors. Moran's I statistic calculation was used to confirm the presence of spatial residual autocorrelation. To identify the type of spatial dependence, tests based on Lagrange Multipliers were calculated. In the case of the Spatial Error Model, the statistical significance of the spatial coefficient λ was verified. To compare the spatial model with the OLS model, AIC and RMSE statistics as well as the correlation coefficient between empirical data and predicted values were used.

2. Ground vibration attenuation relationship and modelling the spatial interaction

The most commonly used model takes into account the values of the PGA (or PGV) according to formula (1). The structural parameters of the model are usually estimated using the least-squares method (OLS). Then the model is statistically verified for the significance of its parameters.

$$\widehat{\log a_{\max,i}} = \alpha_0 + \alpha_1 \log E_i + \alpha_2 \log R_i + \alpha_3 R_i + u_i \tag{1}$$

where: $a_{\max,i}$ – peak values of ground vibration accelerations [m/s^2]; α_0, α_1, α_2, α_3 – structural parameters of the model; E_i – tremor energy [J]; R_i – epicentral distance [m]; u_i – residuals of the model.

In the next stage, the properties of the residual component of the model are examined in terms of normality and homoscedasticity. The lack of sphericity of the random component makes the parameter estimators of the linear regression model inefficient in the class of linear and unbiased estimators. In practice, heteroscedasticity may mean that as the level of values of

648

explanatory variables increases, the values of residuals increase, which in turn translates into an increase in forecast error [22]. In the face of the non-spherical random component, the weighted least squares method can be used to estimate the structural parameters of the model or estimate the model according to the approach using estimators consistent with heteroscedasticity [28]. Another way of dealing with non-sphericity of the residual component is to use non-classical statistical methods which make it possible to verify the assumptions of parametric methods, especially when the exact distributions of the variables on the basis of which the models are estimated are unknown [29].

Apart from the heteroscedasticity of the random component, the phenomenon of spatial clustering of similar residuals can be observed.

To implement spatial correlations into the model of vibration attenuation relationship, it is necessary to create their mathematical representation. This is a fundamental issue of spatial modelling. The most commonly used tool for this purpose is the construction of spatial weight matrices.

The starting point for spatial modelling is the maxim contained in Tobler's law, which states that everything is related to everything else, but near things are more related than distant things. This means that as the distance between the objects under analysis increases, the intensity of interactions between them should decrease. Given that the distance between objects (d_{ij}) is measured according to the Euclidean metric, the elements of the interaction matrix will usually be inverse functions of these measures [30]:

$$d_{ij} = \sqrt{\left(x_i - x_j\right)^2 + \left(y_i - y_j\right)^2} \tag{2}$$

$$w_{ij} = \begin{cases} \dfrac{1}{d_{ij}} & \text{for } i \neq j \quad 0 \quad \text{for } i = j \end{cases} \tag{3}$$

where: w_{ij} – elements of the spatial weights matrix; (x_i, y_i), (x_j, y_j) – coordinates of the analysed objects.

The presence of spatial autocorrelation of the residual component is confirmed by a statistically significant value of Moran's I. The global Moran's I statistic for the variable X with values ε_i observed at n different locations is defined according to formula 4:

$$I = \frac{n}{S_0} \cdot \frac{z^T W z}{z^T z} \tag{4}$$

where: n – the number of all studied units; S_0 – the sum of all elements of matrix W; W – spatial weights matrix; z – column vector with elements $z_i = \varepsilon_i - \underline{\varepsilon}$.

The basis for the construction of this spatial model is the classical model of the ground vibration attenuation relationship presented in formula (1). Given that the random component is subject to spatial autocorrelation, it can be written in the following way:

$$u = \lambda W u + \varepsilon \tag{5}$$

$$(I - \lambda W)u = \varepsilon \tag{6}$$

$$u = (I - \lambda W)^{-1}\varepsilon \tag{7}$$

By substituting the residuals of the classical model u_i with the spatiality-related component, the vibration attenuation relationship model (SEM – Spatial Error Model) can be represented according to formula 8:

$$\widehat{\log a_{\max,i}^{SEM}} = \alpha_0 + \alpha_1 \log E_i + \alpha_2 \log R_i + \alpha_3 R_i + \left(I - \lambda W\right)^{-1} \varepsilon_i \tag{8}$$

The OLS is most commonly used to estimate the structural parameters of linear regression models. Estimators specified by this method are consistent, efficient, and unbiased. Unfortunately, this does not apply to spatial models. In the case of SEM models, the variance-covariance matrix of the random component is, by assumption, non-spherical, which implies the inefficiency of determined estimators. Therefore, the question arises as to what spatial model estimation methods to use so that the determined estimators retain their properties. The literature is dominated by the belief that the best method for estimating structural parameters of spatial models is the maximum likelihood estimation [31]. This method was utilised to estimate the parameters of the vibration acceleration attenuation relationship model.

3. Description of the seismometer data

The subject of analysis is seismometric data from a mining area. This area is characterised by a high level of induced seismicity. An important assumption for the application of spatial statistical models is the necessity to register ground vibrations induced by a single tremor at all measurement stations. Due to this requirement, based on the available data set, measurements registered jointly at all analysed stations were selected for analysis, namely 861 registrations caused by 123 strong tremors. Each ground vibration was registered at seven stations. Fig. 1 shows the distribution of tremor's epicentres as well as the location of the ARP surface apparatus. The
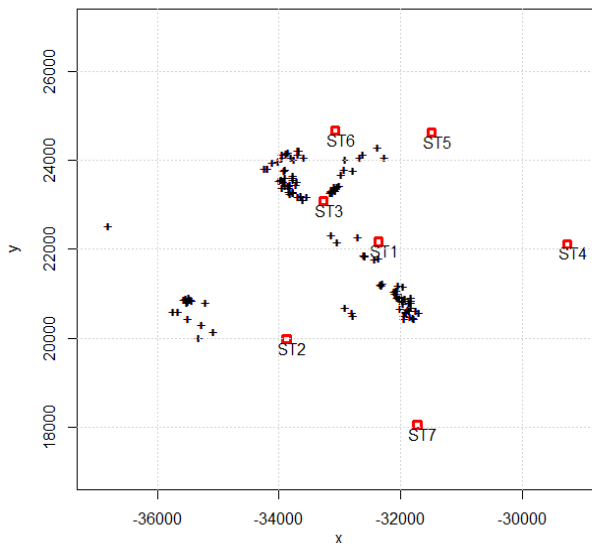
Fig. 1. Distribution of tremor epicentres along with the location of measurement stations

ARP surface apparatus for measuring ground vibration acceleration was located in the vicinity of particularly vibration-sensitive buildings. The localisation of tremors, on the other hand, was carried out using underground seismometer stations, whose location was changed according to changes in the location of longwalls. Mines are obliged to optimise the location of underground seismometer stations when developing mining projects. To determine the speed of propagation of seismic waves, blast tests are performed. However, the location of the z coordinate of the tremor is still subject to significant errors, so in the conducted research, the epicentral distances of the tremors from the position of the ARP apparatus were taken into account.

Table 1 presents basic positional statistics for the distribution of source energy, epicentral distances, as well as vibration acceleration values.

TABLE 1

Basic descriptive statistics of tremor's energy, epicentral distance, and PGA

Parameter	Descriptive statistics				
	Minimum	1st quartile	Median	3rd quartile	Maximum
E [J]	3×10^5	2×10^6	4×10^6	6×10^6	2×10^8
R [m]	224.1	1814.0	2872.5	4038.9	7566.7
a [10^{-3}m/s^2]	2.5	16.7	31.3	78.8	1176.0

The range of energy values for the analysed tremors varied from 3.0×10^5 J to 2.0×10^8 J. The values of epicentral distances varied in the sample from 224 m to 7566 m. The smallest epicentral distances were observed at sites St.1 and St.3 because they were located in close proximity to seismically active regions. On the other hand, the largest values of epicentral distances were observed at sites St.4 and St.7, which were located at the border of the area of tremor. The distribution of logarithms of epicentral distances for the whole analysed sample and for individual measurement stations is shown in Fig. 2. The dominant number of the examined registrations
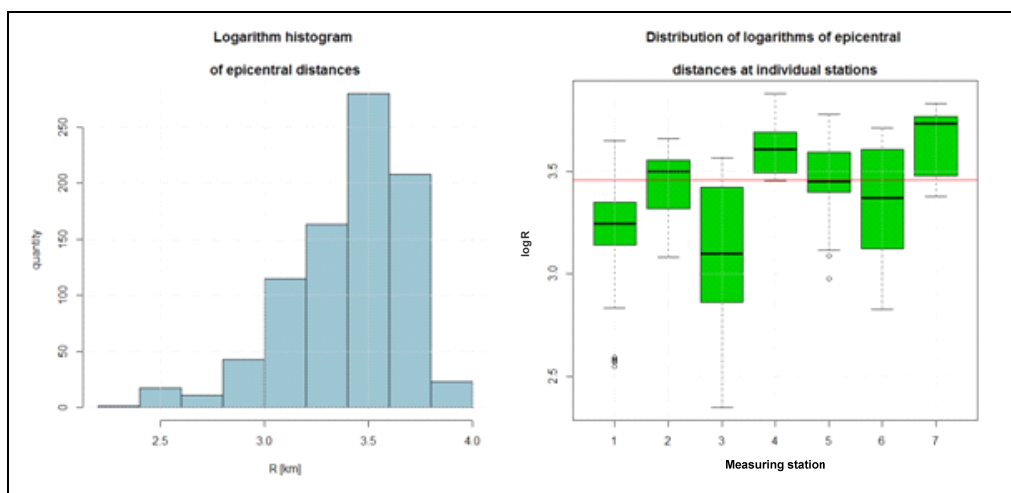
Fig. 2. Distribution of epicentral distances

comes from tremors located in the range from 1100 m to 4800 m (more than 75%) from the measurement stations. Registrations located at distances smaller than 1100 m from the measurement stations represent less than 10% of the analysed seismometric data. The largest epicentral distances (above 4800 m) constitute 15% of the analysed data.

The highest value of PGA (1.176 m/s^2) was caused by a tremor of 7.0×10^7 J energy. Fig. 3 presents the distribution of logarithms of peak ground vibration accelerations for the whole analysed sample and for individual measurement stations. The presented distributions show that the medians of logarithms of PGA at St.1, St.3, and St.6 significantly exceed the general median. On the other hand, at St.4, St.5, and St.7, median values are lower than the general median. The median values of logarithms of PGA at St.2 are very close to the general median. When analysing the distribution of peak ground vibration accelerations, it can be observed that 84% of all resultant horizontal components did not exceed 0.15 m/s^2, while more than 92% did not exceed 0.3 m/s^2. It was found that only 3% of the examined resultant PGA exceeded the value of 0.6 m/s^2, and only 0.8% exceeded the value of 0.9 m/s^2. In terms of the duration of vibration accelerations, more than 73% of the registrations exceeded 3 s.
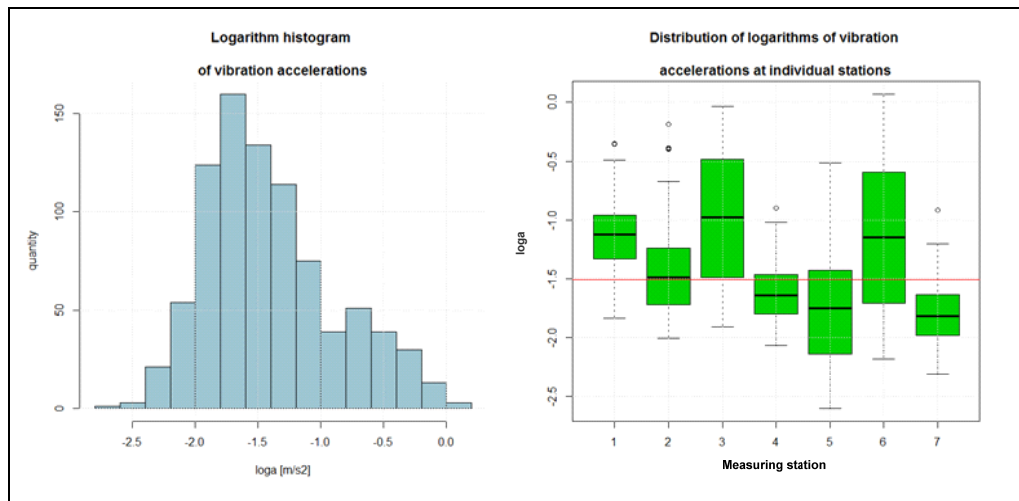
Fig. 3. Distribution of logarithms of PGA

4. Spatial vibration attenuation relationship model

The ground vibration attenuation relationship model was determined for the recorded ground vibration cases. The estimation and evaluation results of the model are presented in Table 2. In all presented tables the significance level of the estimated parameters is shown as follows: (***) means the significance on the level 0.001; (**) – 0.01 and (*) – 0.05. The exact p-value is given if the significance level exceeds the value of 0.05.

The structural parameters of the model are statistically significant at the level of $\alpha = 0.001$ for the variables $\log E$ and $\log R$ and at the level of $\alpha = 0.01$ for the variable R and the intercept. It is important to note a high level of model match with empirical data. More than 81% of the

TABLE 2

Model of vibration attenuation relationship with verification and evaluation

Parameter	$\log E$	$\log R$	R	α_0	F	R^2	AIC	RMSE
Parameter value	0.378 (***)	−1.304 (***)	−0.000045 (**)	0.675 (**)	1259 (***)	0.815	−129.21	0.2237

variation in the logarithms of vibration acceleration was explained by the model. The mean square error of the model is 0.2237. The properties of the residual component of the model were examined in terms of normality and homoscedasticity using appropriate statistical tests. The results are presented in Table 3.

TABLE 3

Test statistics of normality and homoscedasticity of the residuals

Normality of the residual component		Homoscedasticity of the residual component	
Jarque-Bera	Shapiro-Wilk	Breusch-Pagan	White[1]
5.39 (0.06)	0.99 (0.375)	54.37 (***)	60.459 (24.99)

[1] The brackets contain the critical values of test statistics.

In terms of normality of the distribution of residuals, the model meets the assumptions of the Gauss-Markov theorem, yet in terms of the sphericity of the random component, the model is not homoscedastic. Fig. 4 shows the spatial distributions of the residual component of the vibration attenuation relationship model estimated by OLS. The analysed mining area was divided into rasters with dimensions of 150 m by 150 m, and then, for each raster, the average values of residuals were determined. The rasters for which the studied phenomenon was not recorded were removed from the model.

The visual assessment of the distributions of residuals suggests the existence of the phenomenon of spatial autocorrelation. When analysing individual measurement stations, the clustering of the residual component of the log model can be noted. The clusters marked with yellow and red colours denote positive residuals, while grey and black colours denote negative residuals. The existence of spatial autocorrelation of the residual component is confirmed by the areas (clusters) concentrating the residuals with similar values.

For the analysed dataset, the spatial weights matrix for one measurement station has the dimension 123×123. Considering all measuring stations, matrix w_{ij} must be multiplied by the identity matrix within the meaning of the Kronecker. The dimension of the identity matrix results from the number of measuring stations.

For the spatial weights matrix W – based on the inverses of distances between tremor epicentres and given that the column vector z denotes a difference between residuals and the mean of residuals determined based on the log model for individual measurement stations – the value of Moran's I statistic is 0.4387. A graphical method to determine Moran's I statistic is presented in Fig. 5. The graph is divided into four quarters concerning point (0.0). Points located in the first and third quadrants of the system indicate the clustering of units with similar, low or high values [28]. This means the presence of positive autocorrelation. On the other hand, in the second and fourth quadrants, there are points characterised by negative autocorrelation. The x-axis of Moran's I plot presents standardised values of the analysed variable, while the y-axis presents
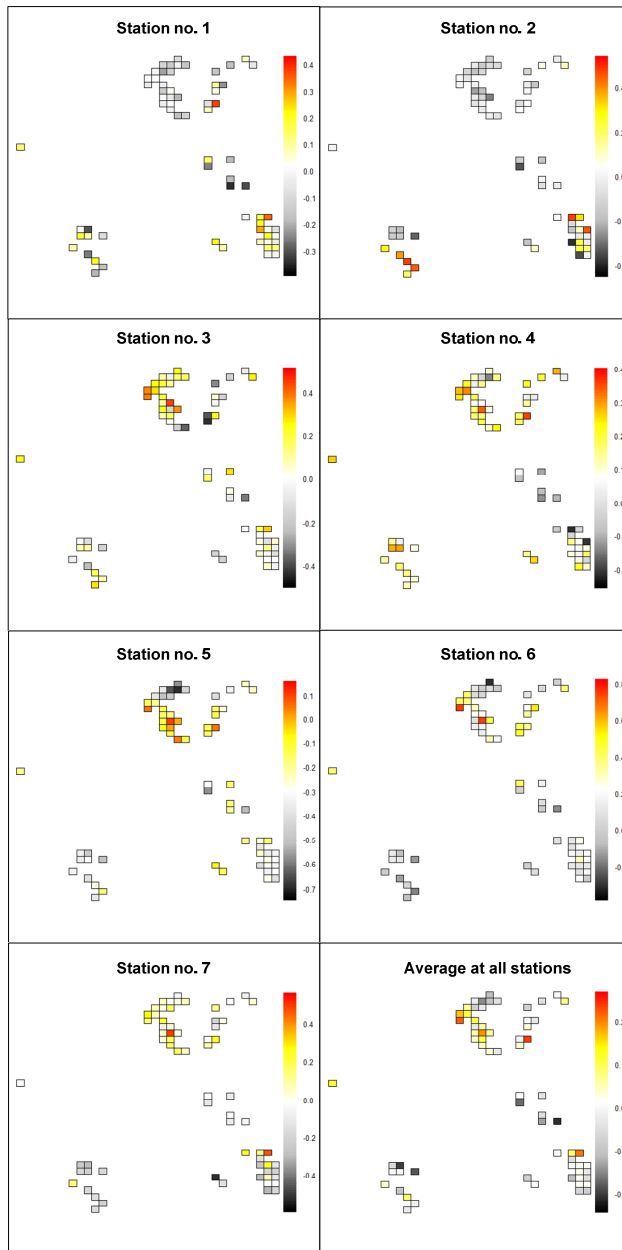
Fig. 4. Spatial distributions of the residual component of the *log* model

standardised values of the spatially delayed variable. The figure shows the number of points belonging to a given quadrant. The regression line is inclined to the OX axis at an α angle with a tangent equaling the value of Moran's I coefficient.
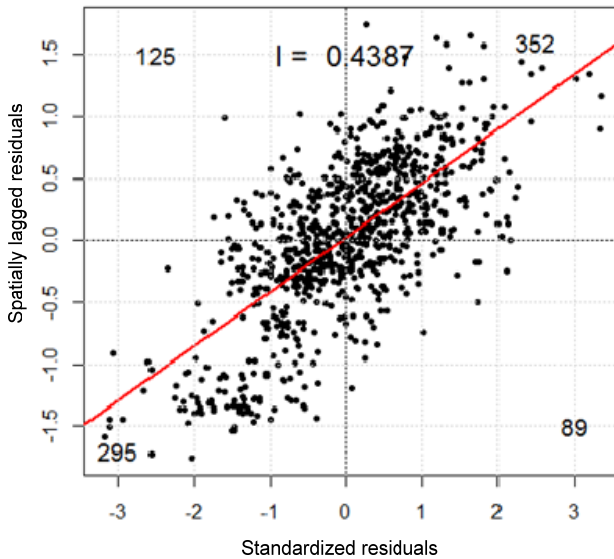
Fig. 5. Point plot of global Moran's I determined from the **W** matrix

The empirically determined spatial interactions in the form of the **W** weight matrix provide a starting point for the construction of spatial regression models. For the diagnostics of spatial dependence, the robust version of the Lagrange Multiplier test was used [31]. The robust LM statistic for the error model is 1266.4$^{(***)}$, while for the auto-regressive model the LM statistic is 6.3944, for which the p-value is 0.02. It means that the spatial error model is more appropriate for describing spatial differentiation.

The maximum likelihood estimation was used to estimate the parameters of the spatial vibration acceleration attenuation relationship model. The results are presented in Table 4. All coefficients of the model are statistically significant at a level of at least $\alpha = 0.05$.

TABLE 4

Estimation results for the spatial ground vibration acceleration model

Parameter	α_0	log$E$	log$R$	R	Lambda
Parameter value	−0.499	0.383	−0.933	-9.8×10^{-5}	0.90128
p-value	(*)	(***)	(***)	(***)	(***)

Table 5 presents the comparison between the spatial model and the classical model. Statistics based on the value of the Pearson correlation coefficient between empirical data and values predicted by the model were used for comparative analyses. In addition, the values of AIC and RSME coefficients for all models were presented, including the level of underestimation and overestimation of the model. This was measured by the maximum value of the residual component, taking into account both positive and negative residuals. All of the above measures were found to favour the spatial model.

Comparison of the match with the empirical data from the SEM model
with the classical ground vibration acceleration model

MODEL	Pearson correlation coefficient	AIC	RMSE	Maximum Model underestimation	Maximum model overestimation
Classical	0.9028134	−129.2115	0.2236992	0.751	0.709
SEM	0.9502013	−614.08	0.1624268	0.571	0.556

In addition, using the spatial model eliminated the autocorrelation of the residual component, as presented in Fig. 6. The Moran's I coefficient for the residuals of the SEM model is 0.0225, and it was statistically insignificant. The residuals of the model show approximate symmetry when considering the different quadrants of the coordinate system. The variance inflation factors for the explanatory variables are 1.065, 7.789, and 7.919 and are less than 10, which is interpreted as no collinearity of the explanatory variables.
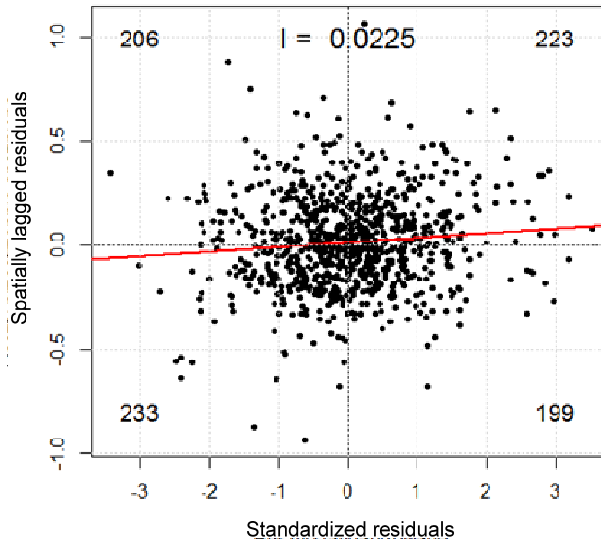
Fig. 6. Moran's I plot for the standardised residuals of the SEM model estimated using the spatial weights matrix W

The Jarque-Bera statistic verifying the residual normal distribution is $17.243^{(***)}$. However, when referring to the central limit theorem, with a large sample, it is sufficient that the random term is asymptotically normal.

The Breusch-Pagan statistic verifying the residual homoscedasticity is $30.541^{(***)}$ and is much lower than for the classical model.

However, an inspection of the residual histogram and the distribution of residuals versus predicted values do not indicate that the assumptions about the properties of the residual component are shaken, which is shown in Fig. 7.

656
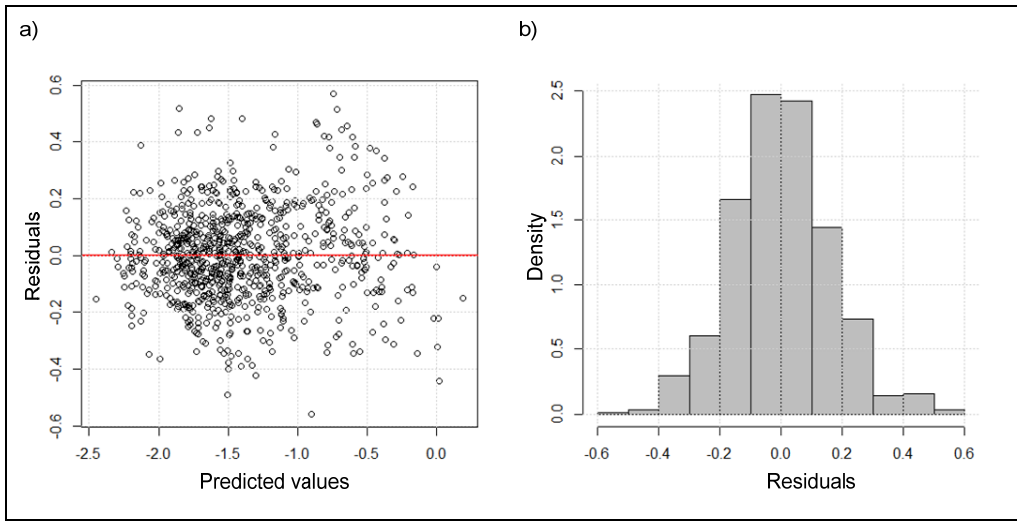
Fig. 7. Residuals properties verification for the SEM model

Fig. 8 shows the comparison of predicted values for both of the estimated models. It is crucial to note a better match for the spatial model, especially on the wings of the distribution of predicted acceleration values.
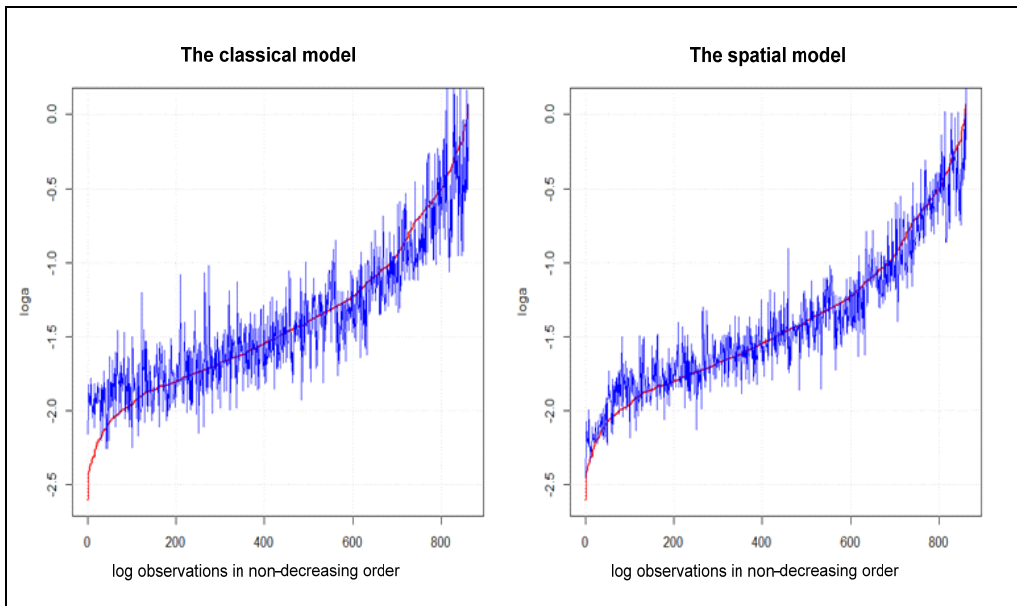
Fig. 8. Comparison of the predicted values estimated by the classical model
with predicted values by the spatial model

By means of the estimated spatial model, the isolines of PGA were determined for the tremor with an energy of 10^7 J. The maps of distribution isolines for accelerations are presented in Fig. 9 and 10. The actual values of accelerations, predictions and relative errors of predictions for the classical and spatial models are presented in Table 6. Bold type indicates values with the module of relative prediction error smaller than when comparing the SEM model with the model estimated by the least-squares method.

TABLE 6

Comparison of predicted values of PGA for the SEM and OLS models along
with relative predicted errors

Station	Actual value	Predicted values		Relative predicted error	
		OLS	SEM	OLS	SEM
	$a \, [\times 10^{-3} \, \text{m/s}^2]$				
1	93.1	123.11	125.47	**−0.32**	−0,35
2	35.9	40.52	39.26	−0.13	**−0,09**
3	567.3	1360.38	912.51	−1.40	**−0,61**
4	40.8	23.85	29.20	0.42	**0,28**
5	44.1	60.71	41.53	−0.38	**0,06**
6	193.8	124.89	173.98	0.36	**0,10**
7	18.2	16.31	15.64	**0.10**	0,14

The percentage average relative errors of PGA predictions are 23% for the SEM model and 44% for the OLS model. This clearly shows that the SEM model prediction describes the distribution of ground vibration acceleration more sufficiently than the OLS model prediction.
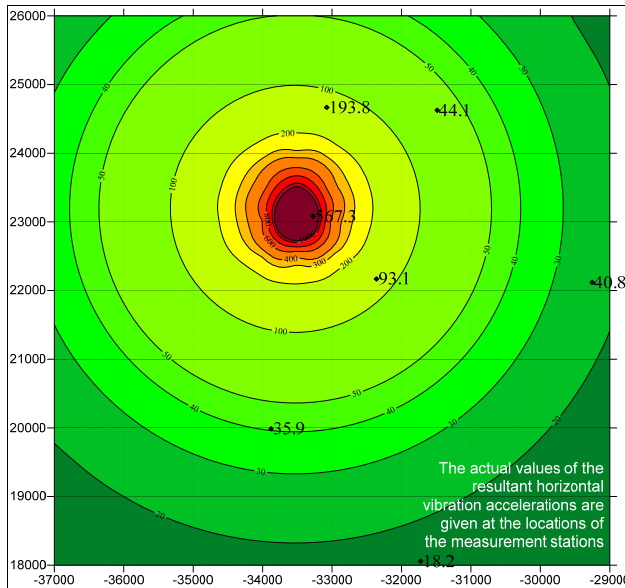
Fig. 9. Isolines of PGA estimated with the OLS model
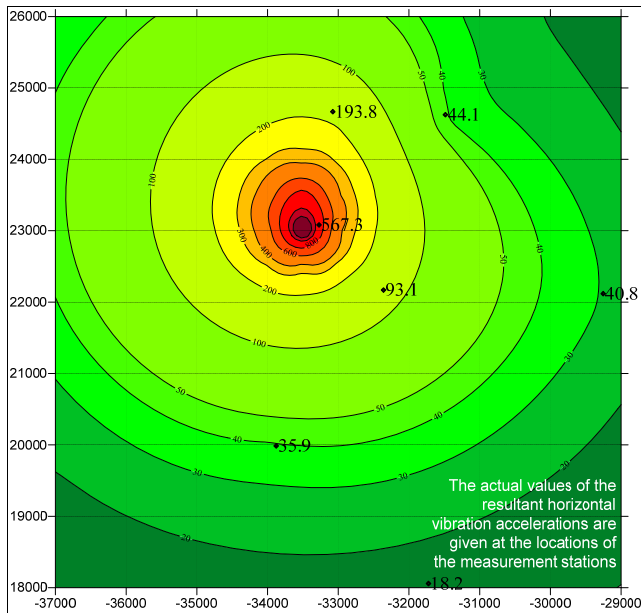
Fig. 10. Isolines of PGA estimated with the SEM model

5. Conclusions

The results of the conducted statistical analysis for the spatial models of peak ground vibration attenuation relationship allowed the Authors to make the following conclusions:

1. The ground vibration attenuation relationship models based on the Joyner-Boor formula with the use of sample limitation to strong phenomena show a very high fit with the empirical data. Unfortunately, in many cases, the classic model overestimates the low values of vibration acceleration while underestimating the high values.

2. Despite a good fit with empirical data, the assumptions of the least squares method are often not met.

3. In light of the heteroscedasticity of the random component, attention was drawn to the spatial nature of the phenomenon of rock tremors.

4. The robust Lagrange Multiplier test was used to indicate the source of the spatial dependence. The SEM (spatial error model) turned out to be the correct model, i.e. a model that takes into account the spatial autocorrelation of the random component.

5. The occurrence of positive spatial autocorrelation of the random component confirms the significant value of Moran's I statistics. This means that areas with similar characteristics clustered around one another, which fully corresponds to the geographical law of Tobler. Moreover, the spatially correlated random component may indicate that the explanatory variables $\log E$, $\log R$ and R do not fully explain the variability of the analysed parameter. It is well known that the factors affecting the intensity of ground vibrations, in addition to the above, are mainly vibration amplification and vibration directivity.

6. The introduction of spatiality into the model in the form of a weights matrix led to an improvement in the quality of the model measured by the coefficients AIC, RMSE and the degree of correlation between the empirical data and the predicted values. The introduction of spatiality also improved the properties of the random component in terms of heteroscedasticity.

7. The application of the SEM model led to the elimination of spatial autocorrelation of the residuals in the sense of the statistical significance of Moran's I coefficient.

8. In this paper, the spatial phenomenon is taken into account using a matrix of spatial weights based on the inverse of the distance between the tremor's epicentres. It seems reasonable to search for other spatial correlations in the form of spatial weights matrices to estimate the model's parameters with an improved match with empirical data and ensure that the assumptions of the least square method are met. An example of this is a weight matrix based on the inverse of distance with "cutoff distance" or the *k*-nearest neighbours. Furthermore, it seems justified to estimate the weight matrix with a structure based on the geophysical parameters of grounds in areas threatened by induced seismicity.

9. The predicted value of the loga parameter is decomposed into a factor related to the trend (Xb) and a factor called the spatial signal ($\lambda Wy - \lambda WXb$). The trend factor explains the variability of the ground vibration intensity parameter in relation to log$E$, log$R$ and R variables. The spatial signal, according to the authors, can be useful in determining factors related to vibration amplification and directivity.

References

[1] Z. Zembaty, S. Kokot, F. Bozzoni, L. Scandella, C.G. Lai, J. Kuś, P. Bobra, A system to mitigate deep mine tremor effects in the design of civil infrastructure. Int. J. Rock Mech. Mining. Sci. **74** (2015).

[2] A. McGarr, J. Bicknell, E. Sembera, R. Green, Analysis of Exceptionally Large Tremors in Two Gold Mining Districts of South Africa. Pure and Applied Geophysics **129** (1989).

[3] H.C. Uzoegbo, K. Li, Mine induced events and its effect on nearby settlements in South Africa. The 14th World Conference on Earthquake Engineering (2008).

[4] J. Dubiński, K. Stec, A. Lurka, Oddziaływanie wstrząsów sejsmicznych na powierzchnię w zależności od ich parametrów fizycznych. Wydawnictwo GIG, Katowice (2005).

[5] G. Mutke, Oddziaływanie górniczych wstrząsów sejsmicznych na powierzchnię. Wydawnictwo GIG, Katowice (2019).

[6] K. Stec (Ed.), Geologiczne przyczyny wzmacniania drgań w nadkładzie serii węglowej na obszarze Górnośląskiego Zagłębia Węglowego. Wydawnictwo GIG, Katowice (2001).

[7] P. Bańka, E. Lier, M.M. Fernandez, A. Chmiela, Z.F. Muniz, A.B. Sanchez, Directional attenuation relationship for ground vibrations induced by mine tremors. J. Min. Sci. **56** (2) (2020). DOI: https://doi.org/10.1134/S1062739120026698

[8] D. Olszewska, S. Lasocki, Relacja tłumienia wartości szczytowej przyspieszenia drgań gruntu z uwzględnieniem amplifikacji dla wybranych rejonów obszaru LGOM. Warsztaty z cyklu Zagrożenia naturalne w górnictwie, (2006).

[9] A. Golik, M. Mendecki, Ground-Motion Prediction Equations for Induced Seismicity in the Main Anticline and Main Syncline, Upper Silesian Coal Basin, Poland. Acta Geophysica **60** (2012).

[10] W.B. Joyner, D.M. Boore, Peak horizontal acceleration and velocity from strong motion records including records from the 1979 imperial valley, California, earthquake. Bulletin of Seismological Society of America **71** (6), (1981).

[11] K.W. Campbell, Near-source attenuation of peak horizontal acceleration. Bulletin of the Seismological Society of America **71** (6), (1981).

660

[12] M. Atkinson, D.M. Boore, Recent trends in ground motion and spectral response relations for North America. Earthquake Spectra (1990).

[13] J. Douglas, B. Edwards, Recent and future developments in earthquake ground motion estimation. Earth-Science Reviews **160**, (2016). DOI: https://doi.org/10.1016 /j.earscirev.2016.07.005

[14] K.W. Campbell, Empirical prediction of near-source and soft-rock ground motion for the Diablo Canyon power plant site, San Louis Obispo country, California. Technical report, Dames & Moore, Evergreen, Colorado (1990).

[15] N.N. Ambraseys, J. Douglas, S.K. Sarma, Equations for the estimation of strong ground motion from shallow crustal earthquakes using data from Europe and Middle East: Vertical peak ground acceleration and spectra acceleration. Bulletin of Earthquake Engineering **3** (1), (2005).

[16] J. Douglas, Earthquake ground motion estimation using strong-motion records a review of equations for the estimation of peak ground acceleration and response spectra. Earth-Science Reviews (2003).

[17] H. Si, S. Midorikawa, New attenuation relations for peak ground acceleration and velocity considering effects of faulty type and site condition. 12th World Conference on Earthquake Engineering (2000).

[18] J. Chodacki, New Ground Motion Prediction Equation for Peak Ground Velocity and Duration of Ground Motion for Mining Tremors in Upper Silesia. Acta Geophysica **64**, (2016).

[19] K.W. Campbell, Y. Bozorgnia, NGA-West2 ground motion model for the average horizontal components of PGA, PGV, and 5%-damped linear acceleration response spectra. Earthquake Spectra **30** (3), (2014).

[20] I.J. Bommer, B. Dost, B. Edwards, P.J. Stafford, J. van Elk, D. Doornhof, M. Ntinalexis, Developing an application-specific ground-motion model for induced seisimicity. Bulletin of the Seismological Society of America (2016).

[21] S. Lasocki, D. Olszewska, Ground motion prediction equations for mining induced seismicity in Legnica Glogow Cooper District in Poland. 16th World Conference on Earthquake, Santiago, Chile (2017).

[22] Ł. Szuła, Statystyczna weryfikacja regresyjnego modelu relacji tłumienia wyznaczonego na podstawie wyników obserwacji drgań gruntu. Przegląd Górniczy **74** (8), (2018).

[23] S. Esposito, I. Iervolino, PGA and PGV spatial correlation models based on European multievent datasets. Bulletin of the Seismological Society of America **101** (5), (2011).

[24] S. Esposito, I. Iervolino, Spatial correlation of spectral acceleration in European data. Bulletin of the Seismological Society of America **102** (6), (2012).

[25] J. Park, P. Bazzurro, J.W. Baker, Modeling spatial correlation of ground motion Intensity Measures for regional seismic hazard and portfolio loss estimation. Applications of statistics and probability in civil engineering. Taylor & Francis Group, London (2007).

[26] J.W. Baker, M. Markhvida, Y. Chen, Progress in measuring spatial correlations in ground motion intensity. Oral Presentation at 17th World Conference on Earthquake Engineering, 17WCEE (2020).

[27] E. Schiappapietra, J. Douglas, Modelling the spatial correlation of earthquake ground motion: Insights from the literature, data from the 2016-2017 Central Italy earthquake sequence and ground-motion simulations. Earth-Science Reviews **203**, (2020). DOI: https://doi.org/10.1016/j.earscirev.2020.103139

[28] K. Kopczewska, Ekonometria i statystyka przestrzenna z wykorzystaniem programu R CRAN. Wydawnictwo CeDeWu, Warszawa (2010).

[29] D. Foszcz, Estymacja parametrów funkcji regresji metodą klasyczną oraz metodami bootstrapowymi. Górnictwo I Geoinżynieria **30** (3/1), 67-78 (2006).

[30] B. Suchecki, Ekonometria przestrzenna. Metody i modele analizy danych przestrzennych, Wydawnictwo C.H.Beck, Warszawa (2010).

[31] L. Anselin, Spatial Econometrics: Methods and Models. Kluwer Academic Publishers, Dordrecht (1988).